Effect of micro-macro crack interaction on softening behaviour of concrete fracture

Syed Yasir Alam, Ahmed Loukili

Effect of micro-macro crack interaction on softening behaviour of concrete fracture

Syed Yasir Alam, Ahmed Loukili

Ecole Centrale de Nantes, L'UNAM Université, Institut de Recherche en Génie Civil et Mécanique (GeM), UMR-CNRS 6183, Nantes, France.

Abstract:

During the fracture of concrete the formation of microcracks is a continuous process where new microcracks are formed in the vicinity of the macrocrack. As the fracture grows, these microcracks interact with the macrocrack and disrupt its smooth opening. In fracture mechanics based approaches; a smooth stress-crack opening softening behaviour is generally used to describe the local fracture process, where the effect of micro-macro crack interactions is lacking. This paper presents firstly an experimental study on the interaction between microcracking and the macrocrack opening (COD) in concrete using digital image correlation and acoustic emission techniques. The study reveals a transient behaviour of macrocrack opening as microcracks are formed in the surrounding. Based on the experimental results, the paper presents a new approach based on Fracture Mechanics to consider the effects of micro-macro crack interaction on the stress-crack opening softening behaviour. Local fracture energy is determined using the new softening model with micro-macro crack interaction for different geometrically similar sizes of the beams and at different locations on the crack profile.

Keywords: fracture; concrete; softening behaviour; crack opening; micro-macro crack interaction; fracture energy

1. Introduction:

Crack growth associated with microcracking is an important phenomenon in fracture process of concrete. Its correct description is very important for the development of appropriate constitutive models. It varies with the size, distribution and type of the constituent materials and involves cracking at several scales (Van Mier, 1997). It consists of main cracks with branches, secondary cracks and a micro fracture process zone ahead of the main cracks. Various micro-defects such as microcracks, dislocations and inclusions, exist in concrete during the process of manufacturing or application. The existing microcracks may propagate and interconnect with the development of new microcracks due to an applied stress. Under tensile stresses, the zone ahead of the macrocrack becomes crowded with microcracks and can be clearly observed using energy based methods e.g. acoustic emission (Haidar, et al. 2005; Landis, 1999; Alam, et al. 2014). These microcracks have very small openings that cannot be directly observed using displacement based methods e.g. digital image correlation

(Wu, et al. 2011; Alam, and Loukili, 2017). Formation of microcracks is a continuous process when the load is increasing. The existing microcracks may open and new microcracks are formed in between the existing microcracks. Mihashi (1987) considered that around the branches of the main crack there are closed microcracks while opening microcracks exist in front of them. Wittmann and Hu (1991) and Hu and Wittmann (1992) however, distinguished an inner interacting microcracking zone from the outside isolated microcracking zone. Since cracking is a major energy sink phenomenon in concrete, the presence of microcracks in the vicinity of the macrocrack may influence its growth, opening behaviour, direction and rate of propagation. The interaction between microcracks and macrocrack is an important phenomenon as it affects the energy dissipation process and thus the fracture behaviour; however, theoretical and experimental works on this topic are very rare in the literature. This paper presents an original experimental study to characterise micro-macro crack interactions.

A tensile softening behaviour comprises of three distinct mechanisms: (1) the growth of microcracks that rapidly coalesce to a macrocrack (2) the progress of the macrocrack that gradually decreases the load carrying capacity of the specimen (3) toughening mechanisms that emanate due to the heterogeneous material structure and the randomly distributed material weaknesses. Many numerical models have been proposed in the literature in order to take into account the different mechanisms based on fracture mechanics e.g. (Hillerborg, et al. 1976; Sancho, et al. 2007) or damage mechanics e.g. (Mazars, 1986; Fichant, et al. 1999). Some coupled continuous-discontinuous models which captured the entire fracture process in concrete are also proposed e.g. (Moonen, et al. 2008; Cuvilliez, et al. 2012; Tamayo-Mas, and Rodríguez-Ferran, 2014; Bobinski, and Tejchman, 2016). In these approaches, fracture is either considered as a discrete macrocrack or a microcracked zone or a microcracked zone leading to a macrocrack. Once a macrocrack is formed, the microcracks nearby can interact with macrocrack and disrupt the smooth opening of the macrocrack. An original experimental investigation is presented in this paper in order to analyse the opening speed of macrocrack at different locations on the crack profile by using of Digital Image Correlation (DIC) technique. It is then correlated with the rate of development of microcracks with the use of Acoustic Emission technique. Further investigation is then performed on the crack opening rate by introducing a new crack opening function within the framework of Fracture Mechanics. The new crack opening function is used to characterise the interaction between microcracks and macrocrack. The initial transient response indicates the oscillatory behaviour of the macrocrack opening. As the crack opening increases, the oscillatory behaviour softens; steady state is achieved when critical crack opening has reached. This experimental study brings a new insight into the softening behaviour of concrete fracture which is commonly used constitutive behaviour in the numerical models.

Another objective of this paper is to present a new cohesive stress - crack opening relation by introducing the effect of micro-macro crack interactions. Within the fracture mechanics framework, cohesive crack modelling (CCM) (Hillerborg, et al. 1976) is the most commonly

used approach to model crack in a continuum. CCM deals with geometrically non-coherent interfaces for which the constitutive relation is expressed in terms of traction–separation laws. Before the activation of the CCM, the cracks act as coherent interfaces capable of capturing elastic resistance to tangential stretch. The issue becomes problematic particularly with increasing cracked area to bulk volume ratios. It is common in the case of fracture of quasi-brittle materials like concrete and mortar; where macrocrack is surrounded by diffused microcracking. In this case, the common approach is to model the developing defects of microstructure as a field of microcracks and smooth variation of stress field (Bažant, and Oh, 1983). However, the interaction of microcracks with the main crack significantly affects the stress redistribution in the vicinity of the macrocrack. Also, since the creation of the microcracked area is a major energy sink in the process of fracture propagation, the micro-macro crack interaction can strongly affect the energy release rate and make characterization of the fracture energy of a quasi-brittle material by classical CCM questionable (Elices, et al. 2002).

Influence of the micro-macro crack interaction on the macrocrack has been researched numerically in few literature works. Kachanov (1985; 1987) and Chudnovsky et al. (1987) proposed a simple solution to cracks interaction problem. The core idea of the method was that the actual tractions on individual cracks were replaced approximately by the average tractions. Based on the complex potentials and superposition principle, Gong and Horii (1989); Gong and Meguid (1992); and Gong (1995) investigated the interaction problem between an arbitrary located and oriented micro-crack and a semi-infinite main crack; Hori and Nemat-Nasser (1987) studied the problem of interaction between micro-cracks and a finite macro-crack. Yan (2005) presented a numerical approach for the interaction problem of macro-crack with micro-crack in an infinite elastic plane. Dayal and Mohammed (1994) found out that as the macro-crack length increased and hence the crack front came nearer to the microcrack, the microcrack had an influence on the stress distribution at macrocrack tip. FEM and XFEM were applied in order to study the effect of micro-cracks on the macro-crack and stress intensity factor (Soh, and Yang, 2004; Wang, et al. 2016; Loehnert and Belytschko 2007).

The aforementioned studies investigated interaction between the macrocrack and microcracks by theoretical methods where macrocrack tip plasticity and cohesive stresses are not considered. In this paper, a new approach to model softening response has been proposed. The parameters of the new model has been investigated and determined experimentally. Local fracture energy is calculated and compared with the RILEM fracture energy. The analysis is performed on two geometrically similar size beams.

2. Material and experimental method:

In this section, the specimen geometries, concrete material properties and experimental procedure of three point bending tests are summarized. Two sizes of concrete beams (designated hereafter as $D1$ and $D2$) with geometrically similar dimensions (length l and

depth D) and one constant dimension (width B) were tested. The cross sectional depths D were 100 and 200 mm respectively with constant width B equals to 100 mm and the span to depth ratio (l/D) equal to 3:1. The beams were notched at mid-span with a notch length a varying proportionally to the size of the beam (a/D was kept equal to 0.2). The design of the beam followed the RILEM recommendation (1990).

The coarse aggregate used in the concrete mixture had a maximum size of D_{agg} equals to 10 mm. The average values of axial compressive strength, indirect tensile strength and the Young's Modulus at 28 days were 58 MPa, 5.76 MPa and 45×10^3 MPa respectively. The three point bending tests were performed with a controlled crack mouth opening displacement (CMOD) rate of 0.2 µm/sec. The fracture test employed a universal testing machine as per RILEM-TMC50 recommendations. Tests were conducted using Instron make 160 kN capacity servo-hydraulic machine under closed-loop crack mouth opening displacement (CMOD) control. Bending tests were performed with a controlled crack mouth opening displacement (CMOD) rate of 0.2 µm/sec using a CMOD clip gauge. One beam of each size was tested. The load, cross-head displacement and CMOD were measured and recorded up to failure using a data acquisition system. The mechanical curves are presented in Figure 1 which shows the characteristic quasi-brittle response of notched concrete beams.

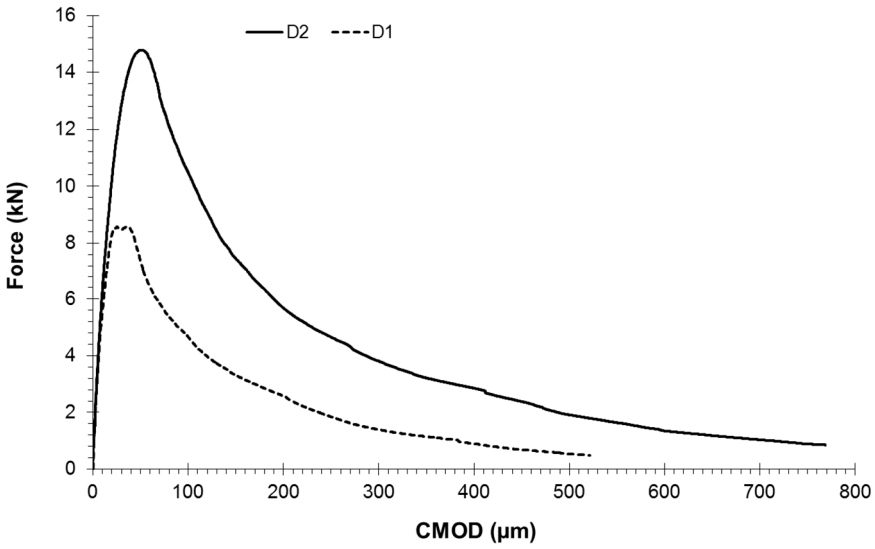

Figure 1. Macroscopic mechanical behaviour of beams

The DIC method was applied and images were obtained continuously during the whole loading branch. Displacement fields were calculated and crack openings were derived. Camera with 50 mm macro lens was mounted in order to image the ligament area above the notch of beam. The digital camera has a resolution of 2452 × 2056 pixels and gives 256 levels of grey output. An area of approximately 80 x 60 mm was captured above the notch for both sizes of beams. At this resolution, the size of pixel is 32 µm which is considered sufficient to perform displacement measurement with 1 µm accuracy (Corr, et al. 2007). The images were taken at a rate of 1 image per second. The images were stored in the system and were analysed afterwards. The correlation of the stored digital images was performed with a

commercial package Vic-2D by calculating the deformation between the reference image and a deformed image. An enhanced correlation algorithm “Zero-normalized squared differences” was used. The subset size was selected as 25x25 pixels and displacement field was determined at each pixel for reliable prediction of displacement fields. Up to peak load the maximum correlation error obtained during the tests was 0.015 pixel which was increased to 0.017 pixel in the post peak loadings. The resolution of the system depends directly on the distribution of grey levels which depends on the texture of the material. A speckle pattern of black and white paint was sprayed on to the surface of specimen to improve the displacement resolution.

Macrocrack propagation in concrete is complex. Vertical and horizontal branches may arise due to aggregate bridging. The meandering and branching of crack are usually difficult to observe using classical DIC as many parameters affect the resolution of the crack observation. Among others, some important parameters are 1) good speckle pattern: it should be carefully done with spots in the range of 3-5 pixels; 2) interpolation scheme for displacement field: in most studies, displacement is calculated by default at steps varying from 5-10 pixels (to reduce computation time) and interpolation schemes are used in between. In this study, displacement field is directly measured using DIC at each pixel; 3) strain smoothing: It is commonly used in the literature; however, it causes loss of local information and is not used in this study. It should also be noted that in most literature work horizontal strains are used to show the crack profile (Wu, et al. 2011; Guo, et al. 2017), which only show the vertical cracks and neglects the branches and deflection of the crack in horizontal direction. However, other techniques e.g. X-ray Computed Tomography (Skarżyński, and Tejchman J., 2016; Huang, et al. 2015) are able to show the horizontal and vertical branches. In this present study, principal strains are used to show the crack profile. Displacement field and continuum mechanics principles were used to calculate the principal strains e.g. as shown in Figure 2.

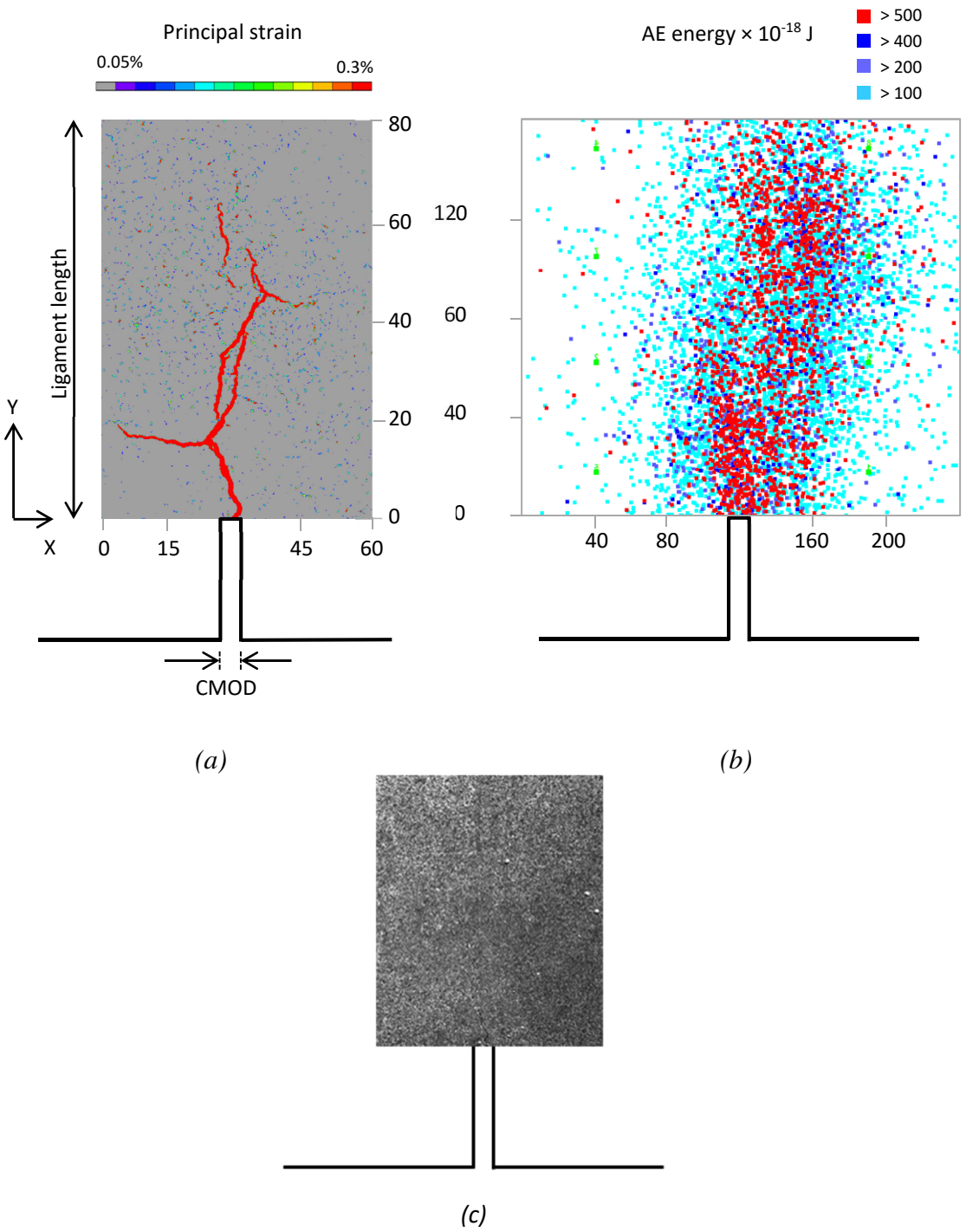

Figure 2. Macrocrack and microcracks pattern in D2 beam using DIC and AE techniques (a) principal strain (b) AE sources (c) specimen surface before DIC and AE analysis.

Crack opening in concrete is a critical parameter; in nonlinear fracture models fracture energy dissipation is directly related to the opening of cracks. Crack opening displacements are measured on the surface of beams from displacement fields by DIC technique (Alam, et al. 2014). For each loading interval, crack opening displacements are measured at different heights (Y location) along the crack profile. Figure 2a shows the principal strains map

obtained from the displacement field. In the following analysis, parameter α (= Y location from notch tip / ligament length) is used to represent position where COD is calculated.

The AE system comprised of a general-purpose interface bus (2 × PCI-DISP4 having 4 channels each). A 3D analysis is performed for the localization of AE events, for which 8 piezoelectric transducers of type R15a were used; all having same frequency range of 50-200 kHz and the same resonance frequency of 150 kHz. The transducers were placed around the expected location of the fracture process zone (FPZ) to minimize errors in the AE event localization. They were placed on both sides of the specimen with silicon grease as the coupling agent. Thus, the sensors form a parallelogram grid location on one side of (60 × 150 mm) for D1 beam and (130 × 150 mm) for D2 beams. The detected signals were amplified with a 40 dB gain differential amplifier. The recorded AE amplitudes ranged from 0 to 100 dB. In order to overcome the background noise, the signal detection threshold was set at a value of 35 dB slightly above the background noise. The hit definition time and hit lockout time used during the tests were set at 200 µsec and 300 µsec respectively. The acoustic wave propagation velocity measured in our study was 5200 m/sec. The acquisition system was calibrated before each test using a pencil lead break procedure. Location accuracy is measured in the range of 5 mm by applying the pencil load fracture at a known location of the specimen.

The localization map of AE sources or events detected during the loading test in concrete beams is presented in Figure 2b. It can be noticed that both DIC and AE show different crack patterns. DIC is an optical technique and measures the crack pattern using displacement discontinuity, thus microcracks are difficult to observe. On the other hand, AE measures location of crack on the basis of energy dissipation (which may be due to sliding, dislocations, opening, rotation, microcracking, kinking, aggregate interlock etc). Many experimental studies have shown that the scattering zone of AE high intensity sources can characterize the microcracking in concrete (Alam, et al. 2014; Haidar, et al. 2005). Also the number of AE sources detected and the measured voltage transient can be related to the microcrack volume in the material through a series of deconvolution (Landis, 1999). AE is generally able to detect small energy dissipations due to microcracks but the location calculation may be undermined due to various reasons e.g. change in AE wave velocity as the material damages. Thus the calculation of width of FPZ may not be objective when macrocrack appears. AE hits data and AE energy dissipation rate are thus used to indicate the loading steps where microcracking is active.

3. Experimental results

3.1. Macrocrack growth with loading

Macrocrack growth with loading can be observed in Figure 3. The macrocrack appear as the initial distributed microcracks localise. These microcracks are difficult to observe but can be characterised using acoustic emission technique (discussed in 3.2). Considerable crack

opening and high strain localisation is generally observed on the macrocrack. In this study the macrocrack is initiated at 40% F/F_{max} in the pre-peak loading regime as shown in Figure 3. Literature review also shows similar results that macrocrack is generated before the peak loading (Wu, et al. 2011; Guo et al. 2017). Some microcracks are also visible before the macrocrack appears. The width of microcracked zone is estimated to be about 40 mm, however, the width of strain localisation zone is about 3 mm. The macrocrack propagates vertically into the specimen as the loading increases. Crack branching, inclined cracks, aggregate interlock and tortuous crack profile can be noticed, which are the characteristic features of crack propagation in concrete. Up to peak load, significant crack penetration occurs into the specimen. The crack growth is progressive; however, as the loading crosses the peak load level, the crack advances rapidly into the specimen. This unstable crack propagation is due to post-peak quasi-fragile behaviour of concrete.

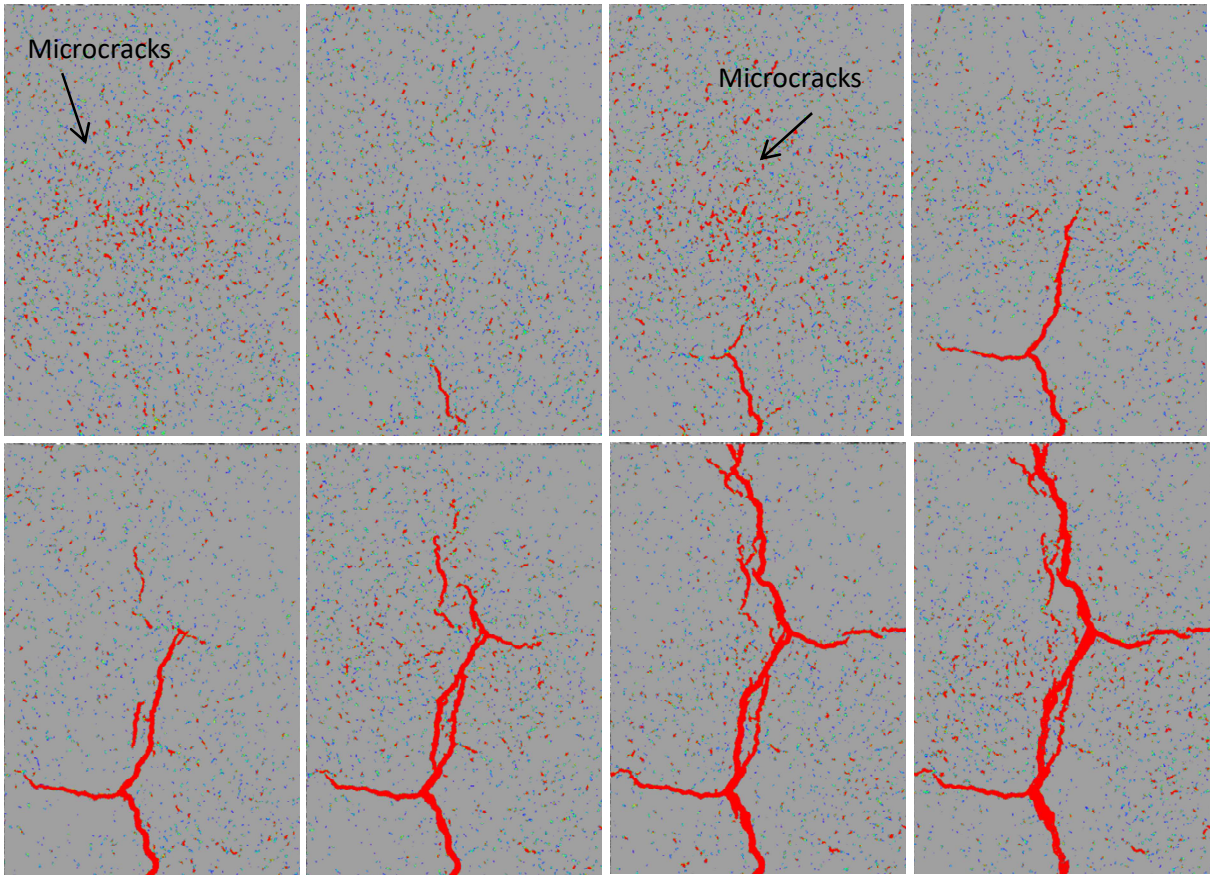

Figure 3. Macrocrack growth in D2 beam at 30% pre-peak, 40% pre-peak, 50 pre-peak, 80% pre-peak, 95% pre-peak, peak, 70% post-peak and 50% post-peak loadings. The coloured pattern shows principal strain field

3.2. Evolution of macrocrack opening and microcrack growth

It can be seen in Figures 2 and 3 that fracture in concrete is characterised by (1) macrocracking characterised by crack openings and elevated strains resulting high energy release and (2) distributed microcracking exhibited by relatively low energy AE sources and

extremely low crack openings usually not in the range of DIC technique. The evolution of both can be obtained from the experimental techniques applied in this study as shown in Figures 4, 5 and 6. Figure 4 presents the evolution of crack openings with the increase in CMOD. The crack opening is calculated by the jump of horizontal displacement across the crack. The crack location was determined at first using principal strains as shown in Figure 2a. The crack locations are then selected i.e. α where CODs were measured. α represents the ratio between Y location from notch tip and ligament length. Two phases of crack opening can be noticed. Initially, the crack openings are very small, however, in the second phase a linear relationship can be noticed between COD and CMOD. It indicates that during the microcracking phase, the crack openings are very small. After the coalescence of microcracks or the formation of macrocrack, the relationship between crack openings and CMOD is essentially linear. This is observed at all the three Y locations considered in this study and in both sizes of the beams.

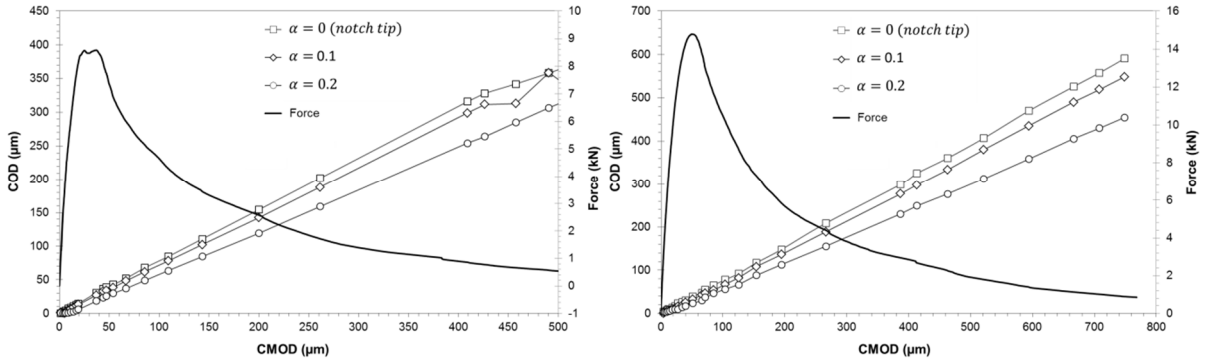

Figure 4. Evolution of crack openings in D1 and D2 beams

* α = Y location from notch tip / ligament length.

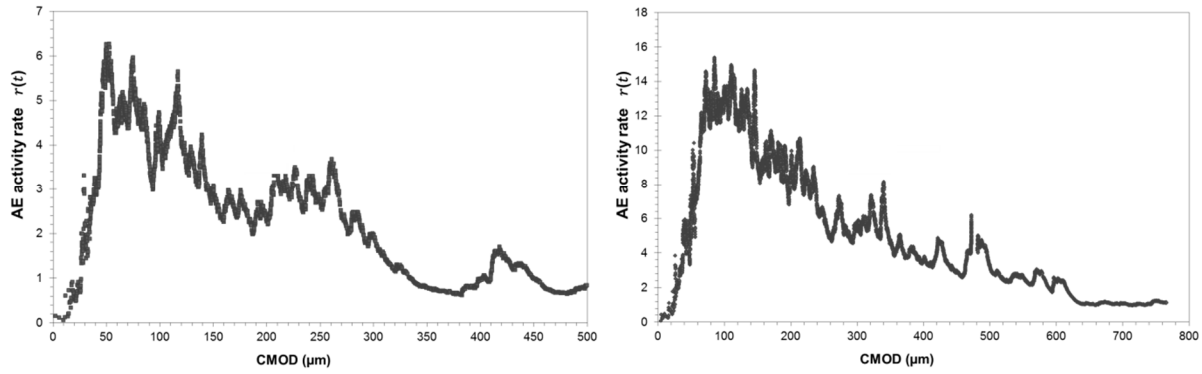

Figure 5. AE activity rate in D1 and D2 beams

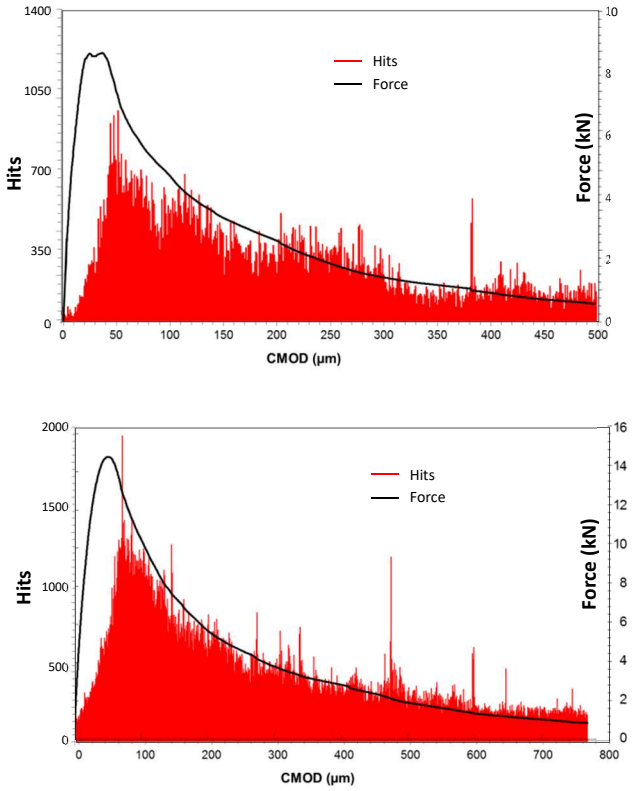

Figure 6. AE hits distribution in D1 and D2 beams

As the loading increases, the number of AE events (N) increases initially. During the initial loadings, the AE activity is very low. Afterwards, a smooth increase in N can be observed due to progressive increase in the damage. Nevertheless, the number of events is generally affected by the number and distance of crack from sensors. Thus, rate analysis of AE activity is performed as shown in Figure 5. AE activity rate $r(t)$ is computed by counting number of AE events $N(t) = \int_0^t r(t)dt$ over a very small interval of time dt corresponding to a very small increment of CMOD ($d\ CMOD$). Figure 5 presents the AE activity rate or simply the rate of development of new microcracks during the fracture process of concrete beams. During the initial loadings, $r(t)$ is very low. Due to progressive microcracking in concrete, $r(t)$ increases due to increasing rate of microcracks formation. After the coalescence of microcracks or the formation of macrocrack, the microcrack rate starts decreasing as shown by the decreasing segment of $r(t)$ – CMOD curve in both beams. Similar behaviour can be observed in Figure 6 where AE Hits distribution is plotted. The number of hits corresponds to number of times AE transient waves generated by the damaging material and received by the AE sensor. AE hit is a useful parameter in the sense that even low damage activity i.e. microcracking produces hits. Therefore, by using hits, one may characterise the microcracking activity before the macrocrack appears. It can be seen that even before the macrocrack appears (F/F_{max} < 40%), some microcracks are produced. These microcracks would dissipate very low energy and may have very low crack openings as shown in Figure 3.

3.3. Transient and steady state behaviour of local crack openings:

Crack advances and opens by an incremental CMOD which means loading is applied at the top face of the specimen such as the mouth of the crack is opening at a constant rate, however, the local crack opening (COD) at each location on the crack profile may behave differently (1) due to cohesive stress between the two lips of the crack which leads to a low crack opening rate as compared to CMOD rate (2) due to interaction with existing and newly formed microcracks around the macro-micro-cracked zone which may cause an erratic behaviour of the crack opening. The (2) behaviour is generally not easy to notice as the measurements of crack openings are usually taken with reference to un-stressed state. The behaviour however, can be observed by plotting the local crack opening speed or rate (ξ) as shown in Figure 7. It can be determined by the ratio between the change in local crack opening ($d\ COD$) with respect to the increment of crack mouth opening ($d\ CMOD$) as follows:

$$\xi = \frac{d\ COD}{d\ CMOD} \tag{1}$$

where $d\ CMOD = CMOD_j - CMOD_i$; i, j are two neighbouring loading states. $d\ CMOD$ is fixed here as digital images were taken each 1 sec which corresponds to $d\ CMOD$ equals to 0.2 µm.

Figure 7 allows us to observe the response (rate of change of COD) by applying an incremental CMOD. The behaviour shows two regimes: an initial transient regime and a final steady state regime. For each location on the crack profile and for each beam, the behaviour is almost identical. In the initial transient regime, COD speed is not constant and shows an erratic or oscillatory behaviour. Significant variation in the COD speed can be observed in this regime. Due to the cohesive stresses between the lips of the crack, COD speed is always smaller than the CMOD speed which was maintained constant throughout the test. It is difficult to measure precisely the beginning of the oscillations with respect to the global force-CMOD/deflection diagram. These oscillations are the result of the interaction between local macrocrack opening and microcracks growth in the vicinity. These interactions are occurring throughout the crack profile where microcrack is partially open and microcracks are forming. As the microcracks growth slows down, the oscillations start reducing. Figure 7 illustrates the transitory behaviour with respect to overall loadings. It can be observed that these oscillations mostly occur during the pre-peak loadings up to peak load i.e. during stable crack propagation. The transient behaviour stabilizes as the loading is reached near the peak (100%). During the second phase or hereby called steady state, the relationship between COD increase and CMOD increment becomes essentially linear. The boundary effect should also be noticed on the behaviour i.e. COD speed is slower when Y location increases. It means when the crack position reaches close to the back face of the specimen, the local crack opening rate slows down due to the boundary effect.

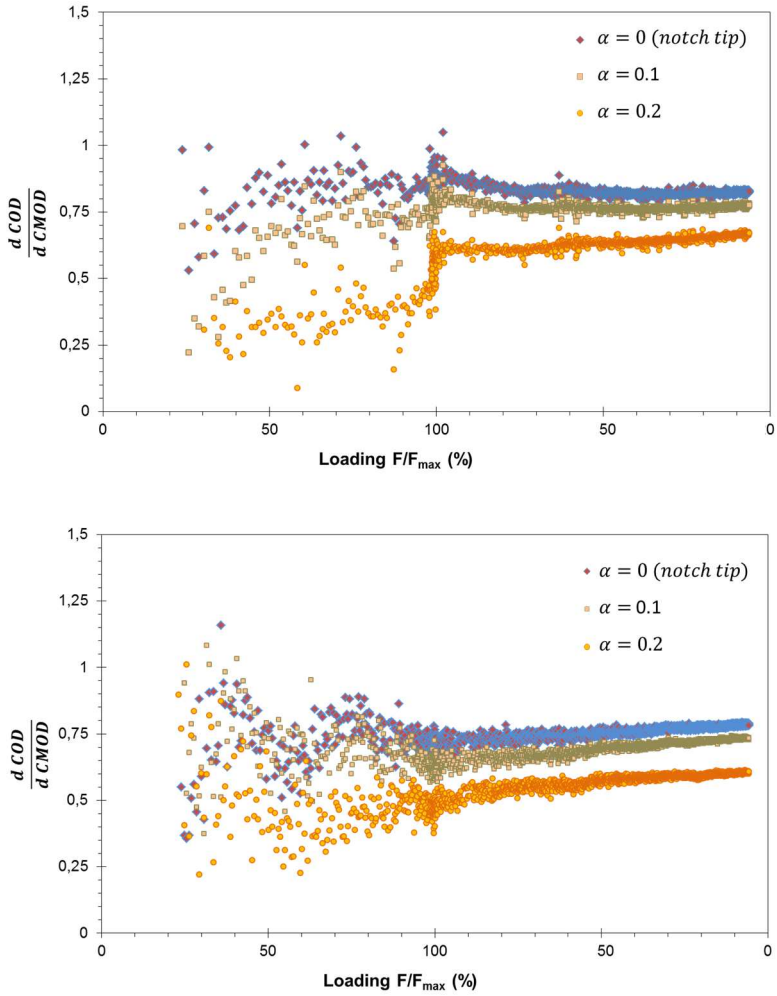

Figure 7. Transient and steady state behaviour of crack opening speed at different locations along crack profile in D1 and D2 specimens.

3.4. Crack opening analysis using Fracture mechanics:

According to linear elastic fracture mechanics (LEFM) when a crack is formed in a body, stress concentration develops around the crack tip. However, in quasi-brittle materials such as concrete and rock, the presence of non-negligible fracture process zone significantly disrupts the stress concentration and LEFM becomes no longer applicable. Hence, nonlinear fracture theories must be used to describe the fracture behaviour of quasi-brittle materials. Among these, the equivalent-elastic crack approach is based on the equivalence between the effective-elastic crack and the linear elastic crack. The effective elastic crack length corresponds to the length of crack which, in a purely elastic model, produces the same compliance to that experimentally observed, i.e., resulting from actual crack. The distance between the tip of the actual traction-free crack a_0 and the tip of the effective elastic crack a_c when the FPZ is fully developed (critical size) is equal to a given characteristic length Δa_c.

$$\Delta a_c = a_c - a_0 \tag{2}$$

In two parameter fracture model by Jenq, and Shah, (1985) based on equivalent elastic crack approach, at the critical loading state the crack opening displacement COD_c at the tip of the crack can be related to crack mouth opening displacement $CMOD_c$ as following:

$$COD_c = CMOD_c \; g\left(\frac{a_c}{b}, \frac{a_0}{a_c}\right) \tag{3}$$

Where g is geometric constant and for different specimens it can be found in an LEFM handbook.

In the following, a new crack opening function is proposed based on equivalent linear elastic crack approach. In order to take into account the interaction between microcracking and macrocrack opening, the new crack opening function takes use of the ratio $COD/CMOD$.

The Equation 3 can be rewritten as:

$$\left(\frac{COD}{CMOD}\right)_c = g\left(\frac{a_c}{b}, \frac{a_0}{a_c}\right) \tag{4}$$

These above equation shows that when material approaches the critical loading condition, the ratio $COD/CMOD$ becomes a constant.

It has been observed in the previous section (3.3) that crack openings initially show the behaviour of transient nature. This behaviour has occurred during the pre-peak loadings where the microcracks growth is active and CODs are very small. During this phase, the COD speed shows cycles of abrupt increase and decrease, however, as loading increases softening of the transient behaviour is observed. The COD speed converges to a constant value. The COD speed convergence indicates stable state behaviour with no COD acceleration until the complete failure occurs. The behaviour confirms Equation 4 and the convergence value observed can be related to the geometric constant on the right hand side of the equation.

Once the critical loading state is achieved, Equation 4 can also be written for two neighbouring loading states as following:

$$\left(\frac{COD}{CMOD}\right)_j - \left(\frac{COD}{CMOD}\right)_i = g\left(\frac{a_c}{b}, \frac{a_0}{a_c}\right)_j - g\left(\frac{a_c}{b}, \frac{a_0}{a_c}\right)_i \tag{5}$$

or

$$\frac{COD_j}{CMOD_j} - \frac{COD_i}{CMOD_i} = \bar{\xi}_{i,j} \tag{6}$$

where i, j are two very close neighbouring loading states at the critical loading condition. $\bar{\xi}_{c\,i,j}$ is a geometric constant and its value should be equal to zero for very small interval between the loading states i and j situated at the critical state.

The new local crack opening function ($\bar{\xi}$) can now be plotted for different locations along the crack profile versus local crack opening displacement (COD) at the same location as shown in Figure 8. $d\ CMOD = CMOD_j - CMOD_j$ is fixed and equals to 0.2 µm. It can be observed that there is an initial transient phase and a final steady phase. The transitory response of $\bar{\xi}$ decreases as COD increases or the so called dampening of $\bar{\xi}$ occurs. The softening of the transient behaviour can be easily observed at all locations on the crack and in all beams. It can be said that the behaviour is almost identical for all cases.

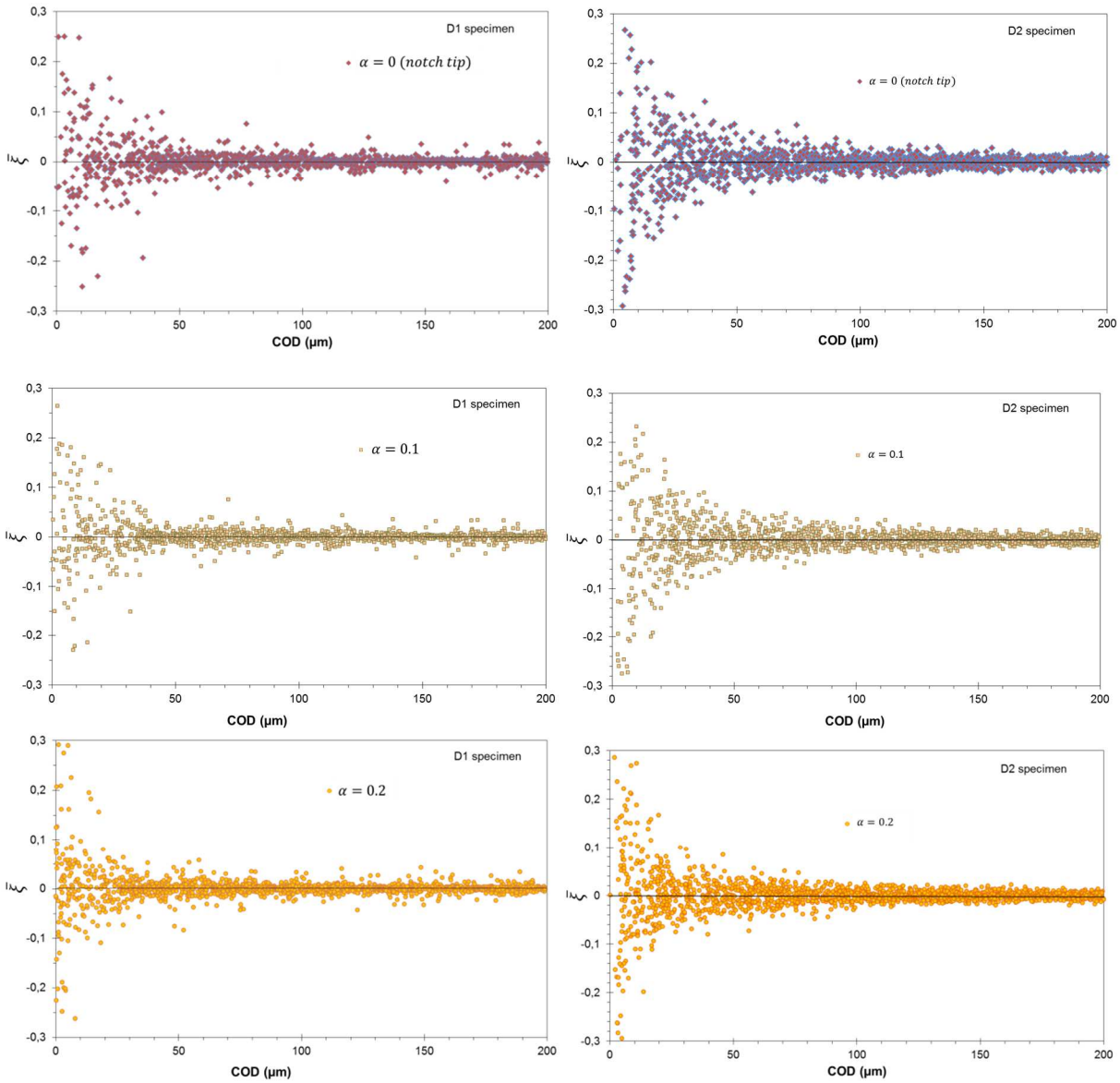

Figure 8. Softening behaviour of local crack opening function ($\bar{\xi}$) at different locations along crack profile in D1 and D2 specimens.

4. Discussion of experimental results and regression analysis

Transitory behaviour is a local phenomenon and is presented in Figure 8 with respect to local COD. The oscillations begin as soon as the COD occurs i.e. when the stress level at the local material point reaches material tensile strength. The amplitude of oscillations then decreases as COD increases. The transient response of crack openings is related to the formation of new microcracks and their interaction with the macrocrack. It is characterized by the stretching and relaxation of macrocrack which can be observed in Figure 8 by +ve and –ve values of function $\bar{\xi}$. The +ve value of $\bar{\xi}$ means increase in the crack opening speed (stretching of macrocrack) during the current incremental increase in CMOD, as compared to the previous step. This is due to development of stresses on the macrocrack and existing microcracks in the surrounding. However, the –ve value of $\bar{\xi}$ means a decrease in crack opening speed (relaxation of macrocrack) during the current incremental increase in CMOD, as compared to the previous step. This is due of the formation of new microcracks in the surrounding which leads to the relaxation of stresses on the macrocrack.

Fracture in quasi-brittle materials initiates by appearance of microcracks in the high stressed zone because of random distribution of mechanical properties, weaknesses and pores. The microcracks are at first distant from each other and opens upon loading. When the loading increases new microcracks are formed in between the already existing microcracks causing relaxation of the later. Upon further loading, the new microcracks also open along with the existing microcracks. Again new microcracks are formed while the microcracking zone begins to localize. The density of the microcracks increases in the microcracked zone until the coalescence of the microcracks to form a macrocrack. The process involves fluctuations of stress-strain behaviour in the microcracked zone due to cycles of opening of existing microcracks and the formation of new microcracks. Macrocrack in the vicinity would be affected by this stress fluctuation. It can be observed in Figure 8 where the macrocrack opening function $\bar{\xi}$ varies in cycles from +ve value to –ve value when microcracking is very active in the surrounding. The behaviour actually shows two regimes: an initial transient regime and a final steady state regime. The transient behaviour softens as crack opening increases. During this phase, the interaction between microcracks and macrocrack is active and affects the macrocrack opening as measured by DIC technique. When crack opening approaches a certain critical value, the behaviour enters into a steady state condition where crack opening grows at a constant speed (traction free crack). This critical crack opening displacement is considered as a characteristic parameter in linear elastic fracture mechanics based models e.g. two parameter model and cohesive zone model. The steady state behaviour characterises the complete coalescence of the microcracks to form a traction free macrocrack. During the transition from transient to steady state behaviour, the material progressively changes from continuum to dis-continuum and the energy dissipation rate becomes higher as noticed by AE technique. It is can be seen that the behaviour $\bar{\xi} - COD$ is similar at each location on the crack for both sizes of the beams. In the forthcoming analysis, this behaviour is considered as characteristic to the material.

The foregoing analysis of crack openings brings new insight into the fracture process of concrete. The transient behaviour of crack openings leads to better understanding of interaction of the microcracks and macrocrack. In a simplest form, the transitory behaviour as observed in Figure 8 can be demonstrated by a damping sinusoidal response as expressed by

$$y = Ae^{-\lambda x}\cos(2\pi f\, x) \tag{7}$$

Where A is the initial amplitude of the envelope; λ is the decay coefficient and f is the frequency or number of cycles per unit.

In this case, λ is the parameter which indicates the softening of the transitory response and can be obtained by performing a regression analysis of the results shown in Figure 9. The initial amplitude A can be directly determined in the Figure 8. The frequency f represents here the number of cycles of loading and unloading of crack per unit crack opening. For both beams the optimum fit parameters has been obtained and are given in Table 1. However, the damping sinusoidal regression curve has been shown in Figure 9 for both beams.

Table 1. Damping sine regression parameters

Beams	A	λ	f
D1	0.3	0.035	0.477
D2	0.3	0.035	0.477

From Figure 9 and Table 1, it can be observed that the regression is not only same for all locations on the crack but it is also same for both beams. Thus the damping regression can be assumed as a characteristic property of the material which shows the transitory behaviour of crack opening due to interaction between microcracks and macrocrack.

The transitory response dampens when the crack opening increases. It attains steady state behaviour when a critical crack opening displacement is reached. From the above analysis, the critical crack opening displacement (COD_c) can be obtained in two steps: (1) calculate the average of +ve and –ve values of COD function ($\bar{\xi}$) for the assumed steady state branch (2) COD_c is the crack opening displacement when the amplitude of regression curve attains the +ve or –ve values of COD function ($\bar{\xi}$). Table 2 shows the COD_c and average $\bar{\xi}$ values obtained in this analysis for both beams. It can be observed that both beams show almost similar results. The critical crack opening displacement which indicates the onset of the steady state behaviour is same and can be considered as characteristic material parameter.

Table 2. Parameters of critical crack opening displacement

Beams	Average +ve $\bar{\xi}$	Average -ve $\bar{\xi}$	COD_c (µm)
D1	0.00376	- 0.00377	123.6
D2	0.00420	-0.00423	121.5

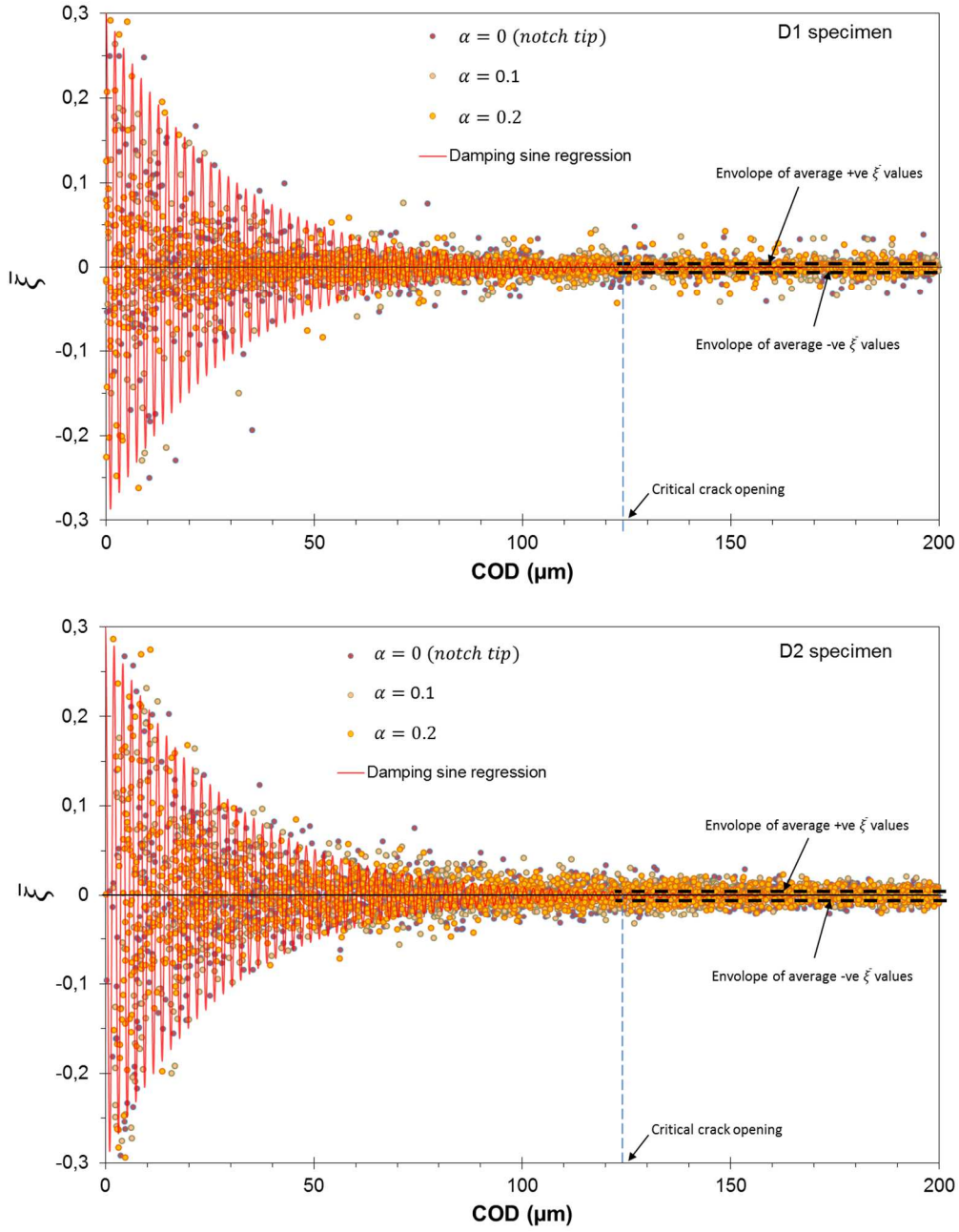

Figure 9. Damping sine regression plot for beams D1 and D2

5. New cohesive crack model with micro-macro crack interaction

The transitory behaviour during micro-macro crack interaction and its effect on the crack opening as presented in this study are generally not taken into account during the modelling of concrete fracture e.g. in case of cohesive crack model. Since the transient response causes the stress-strain fluctuations in the fracture process zone, it would consume some part of the potential energy stored in the structure. Thus it would affect the fracture energy calculation if a classical cohesive crack model is used. From fracture mechanics point of view, the transitory behaviour can be represented by the introduction of a transitory stress σ_ξ

which dampens as the crack opening increases until a certain critical crack opening COD_c has reached as shown in Figure 10.

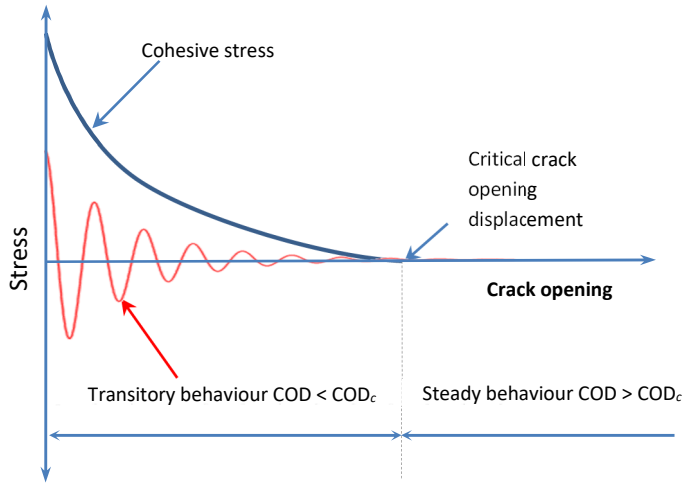

Figure 10. Transitory behaviour with increase in crack opening

In the classical form of cohesive crack model (Hillerborg, et al. 1976; Cedolin, et al. 1987), energy dissipation or fracture energy is determined by a simple linear stress-crack opening relationship.

$$\sigma_c(w) = f_t\left(1 - \frac{w}{COD_c}\right) \tag{8}$$

where $\sigma_c(w)$ is the cohesive stress as a monotonic decreasing function of crack opening (w) and f_t is the tensile strength of the material.

Many other $\sigma_c(w)$ relationships have been proposed in literature. Gopalaratnam and Shah (1985) proposed an exponential curve. It is interesting to note that the transient behaviour of crack openings as shown in Figure 8 and Figure 9 also show exponential softening form. The softening exponential $\sigma_c(w)$ relationship can be given as:

$$\sigma_c(w) = f_t e^{-\lambda w} \tag{9}$$

where λ is the softening parameter as shown in Table 1.

Now the transitory stress from the Equation 7 can be introduced as a damping sinusoidal response:

$$\sigma_\xi(w) = \Psi e^{-\lambda w}\cos(2\pi f w) \tag{10}$$

where $\sigma_\xi(w)$ is the transient stress acting on the crack due to micro-macro crack interaction. The parameters λ and f are the same as determined in section 4. However, Ψ is the initial amplitude of the transient stress.

Now the total stress acting on the face of crack can be expressed as following:

$$\sigma(w) = \sigma_c(w) + \sigma_\xi(w) = [f_t + \Psi \cos(2\pi f w)]e^{-\lambda w} \quad (11)$$

The fracture energy can now be determined as the area under the curve:

$$G_f = \int_0^{COD_c} \sigma(w)\, dw \quad (12)$$

The characteristic length (Hillerborg, et al. 1976) can thus also be calculated as:

$$l_{ch} = \frac{E\, G_f}{{f_t}^2} \quad (13)$$

In order to determine the complete softening curve and to calculate fracture energy, the parameters need to be determined are f_t, Ψ, f and λ. The parameters f and λ can be determined from regression analysis as shown in Table 1. The parameter f_t should be determined from experiment preferably using a uniaxial tensile test. Otherwise, f_t can be roughly taken equal to rupture of modulus using brasilien test. Now the parameter Ψ can be easily determined using the boundary condition $\sigma(COD_c) = 0$.

The fracture energy can now be calculated from Equation 9 for the concrete used in this study. The parameters obtained are given in Table 3. For convergence reasons $\sigma(COD_c)$ is taken as $0.01\, f_t$. where f_t is assumed as the brasilien strength. The fracture energy is in order with the values found in the literature. For both beams same fracture energy is obtained which can indicate that this fracture energy is independent of size of the structure. The stress – crack opening curve obtained is given in the Figure 11. It can be seen that $\sigma(w)$ diminishes as w approaches ∞. Once COD_c is achieved, the remnants of $\sigma(w)$ is due to the frictional resistance between the two crack surfaces.

Table 3. Parameters of new cohesive crack model with micro-macro crack interaction and fracture energy calculation

Beams	f_t (MPa)	f	λ	Ψ (MPa)	COD_c (µm)	G_f (N/m)	l_{ch} (mm)
D1	5.76	0.477	0.035	1.56	123.6	162.2	220.0
D2	5.76	0.477	0.035	1.84	121.5	162.4	220.3

Table 3 presents the fracture parameters obtained purely from experimental study. The finite element modelling of the proposed model is not covered in this paper. The main parameter is the G_f which was determined by applying common boundary condition of cohesive crack model $0 \leq COD \leq COD_c$ (COD_c was determined directly using experimental data) and regression parameters (unique set of parameters were obtained for three different locations on the crack for each beam).

The parameters of transient fracture growth obtained seem to be unique for a material and do not depend on the size of the specimen or the location of the crack. However, studies (Wittmann et al. 1990; Duan, et al. 2003; Duan, et al. 2007) have shown that RILEM fracture energy (based on cohesive zone model) method shows size effect. It should be noted that, this size effect is due to presence of boundary effect on the fracture development. However, if no boundary effects are present, the fracture energy is the characteristic material property (Bazant, and Planas, 1998). In this study however, G_f is considered as a local quantity and the locations where G_f was measured, were away from the boundary (α = 0, 0.1 and 0.2). From literature review, it is realistic to assume that at local scale, the strength is independent of structural size and so is the fracture energy, with the condition that there is no boundary effect. However, the specimen size has an impact on the global structural response which includes post-peak behaviour, overall energy consumption. In fact, local behaviour along with boundary conditions constitutes the response at the structural scale (Van Mier, and Man, 2009). However, in the present paper we focused on the local fracture response and correction between microcracks and local macrocrack opening.

It can be noticed that the transient behaviour always begin with macrocrack's formation. In the framework of cohesive crack approach which is still the commonly used fracture model, macrocrack or displacement discontinuity occurs as soon as the material reaches its tensile strength. Based on the experimental findings and the new cohesive crack model, interactions between microcracks and macrocrack can be determined and added on the softening behaviour of the material. Numerically speaking, the current model can be used in both discrete/discontinuous approaches or by using continuous – discontinuous approach. The numerical modelling of concrete fracture using the proposed cohesive model would be an interesting task which is currently underway.

The cohesive zone model has a convenient mathematical formulation for describing the damage behaviour in the quasi-brittle material. Nevertheless, the classic form of cohesive crack models have some intrinsic limitations linked to the simplified assumptions in the model such as: a localized discontinuity, closed crack condition, non-dissipative condition of the bulk material (Alam, et al. 2017). By introducing the transient behaviour presented in this paper, one can include the effects of material heterogeneity, microcracking and the stress variations in the fracture process zone during its development.

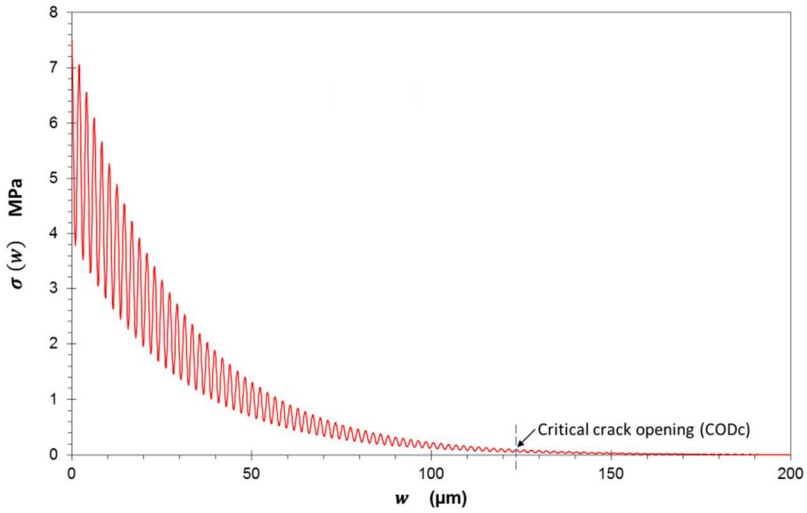

Figure 11. Stress – crack opening curve obtained for D1 and D2 beams using cohesive crack model with micro-macro crack interaction.

Conclusions:

In this paper, a new approach to analyse the crack opening response by taking into account the microcracking in the vicinity is presented. Based on Fracture Mechanics principals, a new crack opening function $\bar{\xi}$ is developed. It can be concluded that the increase/decrease of crack opening function $\bar{\xi}$ at any location on the crack can give insight into the local fracture response from which behaviour of local stresses due to development of fracture process zone can be analysed.

- When loading increases, the crack opening crack opening function $\bar{\xi}$ at any location shows at first a transient behaviour and then a steady state behaviour which is due to the micro-macro crack interaction. The transient response of crack opening function $\bar{\xi}$ is related to the formation of new microcracks and their interaction with the macrocrack. It is characterized by the stretching and relaxation of macrocrack as new microcracks are formed in the vicinity. The transient behaviour involves stress-strain fluctuations in the fracture process zone and results in significant energy dissipation during small crack openings as observed by higher activity rate.
- The transient nature of crack opening function $\bar{\xi}$ softens as the crack opening increases. A steady state is achieved when a critical crack opening has reached where the crack opening function $\bar{\xi}$ approaches to zero. During the steady state regime, the crack opens with a constant rate until the failure occurs.
- The transient behaviour shows the softening response similar to like cohesive crack model. An improved cohesive crack model is presented where a damping transitory stress due micro-macro crack interaction is added to the cohesive stress.
- The parameters of the new cohesive crack model are determined from the experimental results. Fracture energy is calculated and complete stress-crack opening response is plotted.
- Two beams of different sizes but geometrical similar dimensions are tested. The beams show identical behaviour of crack opening function $\bar{\xi}$. The new cohesive crack

model parameters are found to be similar for both beams. Fracture energy calculated from the new cohesive crack model is independent of the size of the beam and location of the crack.

References:

Alam, S.Y., Saliba J., Loukili. A., 2014. Fracture examination in concrete through combined digital image correlation and acoustic emission techniques. Construction and Building Materials 69, 232–242.

Alam, S.Y., Loukili, A., 2017. Transition from energy dissipation to crack openings during continuum–discontinuum fracture of concrete, International Journal of Fracture 206, 49-66.

Bažant, Z.P., Oh, B.H., 1983. Crack band theory for fracture of concrete. Materials and Structures 16, 155-177.

Bažant, Z.P., Planas, J., 1998. Fracture and size effect in concrete and other quasibrittle materials. CRC Press

Bobinski, J., Tejchman, J., 2016. A coupled constitutive model for fracture in plain concrete based on continuum theory with non-local softening and eXtended Finite Element Method. Finite Element in Analysis and Design 114, 1-21.

Cedolin, L., DeiPoli, S., Iori, I., 1987. Tensile behavior of concrete. Journal of Engineering Mechanics ASCE 113, 431-449.

Chudnovsky, A., Dolgopolsky, A., Kachanov, M., 1987. Elastic interaction of a crack with a microcrack array—II. Elastic solution for two crack configurations (piecewise constant and linear approximations). International Journal of Solids and Structures 23, 11-21.

Corr, D., Accardi, M., Graham-Brady, L., Shah, S.P., 2007. Digital image correlation analysis of interfacial debonding properties and fracture behavior in concrete. Engineering Fracture Mechanics 74(1-2), 109-21.

Cuvilliez, S., Feyel, F., Lorentz, E., Michel-Ponnelle, S., 2012. A finite element approach coupling a continuous gradient damage model and a cohesive zone model within the framework of quasi-brittle failure. Computer Methods in Applied Mechanics and Engineering 237–240, 244-259.

Dayal, V., Mohammed, I., 1994. Micro-macro crack interaction in composites. Engineering Fracture Mechanics 49(5), 647-658.

Duan, K., Hu, X.-Z., Wittmann, F.H., 2003. Size effect on fracture resistance and fracture energy of concrete. Materials and Structures 36, 74-80.

Duan, K., Hu, X.-Z., Wittmann, F.H., 2007. Size effect on specific fracture energy of concrete. Engineering Fracture Mechanics 74(1-2), 87-96.

Elices, M., Guinea, G., Gomez, F., Planas, F., 2002. The cohesive zone model: advantages, limitations and challenges. Engineering Fracture Mechanics 69, 137-163.

Fichant, S., La Borderie, C., Pijaudier-Cabot, G., 1999. Isotropic and anisotropic descriptions of damage in concrete structures. Mechanics of cohesive-frictional materials 4, 339-359.

Gong, S.X., Horii, H., 1989. General solution to the problem of microcracks near the tip of a main crack. Journal of the Mechanics and Physics of Solids 37, 27-46.

Gong, S.X., Meguid, S.A., 1992. Microdefect interacting with a main crack: A general treatment. International Journal of Mechanical Sciences 34, 933-945.

Gong, S.X., 1995. On the main crack-microcrack interaction under mode III loading. Engineering Fracture Mechanics 51, 753-762.

Gopalaratnam, V.S., Shah, S.P., 1985. Softening response of plain concrete in direct tension. ACI Journal 28, 310-323.

Guo, M., Alam, S.Y., Bendimerad, A.Z., Grondin, F., Rozière, E., Loukili, A., 2017. Fracture process zone characteristics and identification of the micro-fracture phases in recycled concrete. Engineering Fracture Mechanics 181, 101-115.

Haidar, K., Pijaudier-Cabot, G., Dubé, J.F., Loukili, A., 2005. Correlation between the internal length, the fracture process zone and size effect in model materials. Materials and Structures 38(2), 201-210.

Hillerborg, A., Modéer, M., Petersson, P.E., 1976. Analysis of crack formation and crack growth in concrete by means of fracture mechanics and finite elements. Cement and Concrete Research 6, 773-782.

Hori, M., Nemat-Nasser, S., 1987. Interacting micro-cracks near the tip in the process zone of a macro-crack. Journal of the Mechanics and Physics of Solids 35, 601-629.

Hu, X., Wittmann, F.H., 1992. Fracture energy and fracture process zone. Materials and Structures 25, 319-326.

Huang, Y., Yang, Z., Ren, W., Liu, G., Zhang, C., 2015. 3D meso-scale fracture modelling and validation of concrete based on in-situ X-ray Computed Tomography images using damage plasticity model. International Journal of Solids and Structures 67-68, 340-352.

Jenq, Y. S., Shah, S. P., 1985. A Two Parameter Fracture Model for Concrete. Journal of Engineering Mechanics 111(4), 1227-1241.

Kachanov, M., 1985. A simple technique of stress analysis in elastic solids with many cracks. International Journal of Fracture 28, 11-19.

Kachanov, M., 1987. Elastic solids with many cracks: a simple method of analysis. International Journal of Solids and Structures 23, 23-43.

Landis, E.N., 1999. Micro-macro fracture relationships and acoustic emissions in concrete. Construction and Building Materials 13(1), 65-72.

Loehnert, S., Belytschko, T., 2007. Crack shielding and amplification due to multiple microcracks interacting with a macrocrack. International Journal of Fracture 145(1), 1-8.

Mazars, J., 1986. A description of micro- and macroscale damage of concrete structures. Engineering Fracture Mechanics 25(5-6), 729-737.

Mihashi, H., 1987. States of the art and a view of the fracture mechanics of concrete. Journal of JCI 25(2), 14-25.

Moonen, P., Carmeliet, J., Sluys, L.J., 2008. A continuous–discontinuous approach to simulate fracture processes in quasi-brittle materials. Philosophical Magazine 88(28-29), 281-3298.

RILEM Recommendation, 1990. Size-effect method for determining fracture energy and process zone size of concrete. Materials and Structures 23, 461-465.

Sancho, J.M., Planas J., Cendón, D.A., Reyes, E., Gálvez, J.C., 2007. An embedded crack model for finite element analysis of concrete fracture. Engineering Fracture Mechanics 74(1-2), 75-86.

Skarżyński, Ł., Tejchman J., 2016. Experimental Investigations of Fracture Process in Concrete by Means of X-ray Micro-computed Tomography. Strain 52(1), 26-45.

Soh, A.K., Yang C.H., 2004. Numerical modeling of interactions between a macro-crack and a cluster of micro-defects. Engineering Fracture Mechanics 71(2), 193-217.

Tamayo-Mas, E., Rodríguez-Ferran, A., 2014. A new continuous-discontinuous damage model: cohesive cracks via an accurate energy-transfer process, Theoretical and Applied Fracture Mechanics 69, 90-101.

Van Mier, J. G. M., 1997. Fracture processes of concrete: assessment of material parameters for fracture models. CRC Press, Boca Raton.

Van Mier, J. G. M., Man H.-K., 2009. Some Notes on Microcracking, Softening, Localization, and Size Effects. International Journal of Damage Mechanics 18(3), 283-309.

Wang, H., Liu, Z., Xu, D., Zeng, Q., Zhuang, Z., Chen, Z., 2016. Extended finite element method analysis for shielding and amplification effect of a main crack interacted with a

group of nearby parallel microcracks. International Journal of Damage Mechanics 25(1), 4-25.

Wittmann, F. H., Hu, X., 1991. Fracture process zone in cementitious materials. International Journal of Fracture 51(1), 3-18.

Wittmann, F.H., Mihashi, H., Nomura, N., 1990. Size effect on fracture energy of concrete. Engineering Fracture Mechanics 35(1-3), 107-115.

Wu, Z., Rong, H., Zheng, J., Xu, F., Dong, W., 2011. An experimental investigation on the FPZ properties in concrete using digital image correlation technique. Engineering Fracture Mechanics 78, 2978-2990.

Yan, X., 2005. Microdefect interacting with a finite main crack. The Journal of Strain Analysis for Engineering Design 40, 421-430.